Optimization of Active Control Systems to Suppress Flutter and Minimize Turbulence Response

Carl S. Rudisill*
Clemson University, Clemson, S.C.

A method for optimizing an active control system which will suppress flutter and minimize the response of a lifting surface to atmospheric turbulence is presented. A mathematical search method is developed which will find a control law which will cause an active control system to flutter at a specified freestream velocity, air density, and Mach number. With the flutter velocity of the system held constant, the control law is then modified in such a way that the peak output power spectral density function of the angular response of a lifting surface (as a result of atmospheric turbulence) is minimized for a specified flight velocity which is less than the flutter velocity. The von Karman generalized power spectrum for the transverse components of turbulence is used to find the value of the output power spectral density function of the response. The optimization procedure is used in an example problem to increase the flutter velocity and minimize the turbulence response of a simplified delta-wing model which has leading and trailing edge control surfaces.

Nomenclature

b	= reference semichord
$h(x,y,t)$	= vertical displacement
h_1,h_2	= vertical displacements of accelerometer (Fig. 1)
k	= reduced frequency
L	= scale of turbulence
$\Delta P(x,y,t)$	= pressure distribution
P_i	= control law component
q_i	= generalized displacement of the ith vibration mode
$\bar{q}^T$	= transpose of the complex congugate of the vector q
s	= reference area
t	= time
V	= flutter velocity
V_c	= flutter velocity constraint
V_g	= flight velocity
x,y	= streamwise and spanwise coordinates, respectively
$Z_i(x,y)$	= normalized deflections of the ith vibration mode
α	= angle of attack at section A-A (Fig. 1)
β	= leading-edge control deflection
δ	= trailing-edge control deflection
$\Phi_\alpha(\omega)$	= output power spectral density function
$\Phi_{w_g}(\omega_g)$	= input power spectral density function
ω	= circular frequency of oscillation
ω_g	= circular frequency of gust
ω_i	= undamped circular frequency of ith mode

I. Introduction

Trends in flight structural design in recent years have been toward an increase in flexibility, slenderness ratio, and higher operating speeds. These trends have increased the probability of encountering excessive stresses due to gust loadings and flutter within the aircraft's operating envelope. Requirements to fly higher, faster, and further with larger payloads have resulted in larger and more flexible airframes. With the present trend in aircraft design toward the more flexible vehicles, the reduction of stresses due to gust response and the prevention of flutter of the lifting surfaces is becoming a major consideration in the development of lightweight airframes.

At the present time, flutter problems are solved by modifying the structure, adding mass balance, and establishing suitable flutter placards. These approaches limit performance, payload, and system capability.

It has been demonstrated that active control systems can be designed to alter the dynamic characteristics of large flexible aircraft.[1-3] Analytical studies indicate that active controls for flutter suppression are technically feasible and offer significant structural weight savings.[1,4-6]

Recently, the application of active control technology for the suppression of flutter has been successfully demonstrated by inflight testing of a flutter suppression system on a B-22 airplane,[2,3] and also by wind tunnel tests.[7,8] Recent technological advances in the field of control systems and the increased reliability of control system components make the use of active controls for flutter suppression very attractive.

An active control system is defined here as a feedback control system which consists of a) sensors for the detection

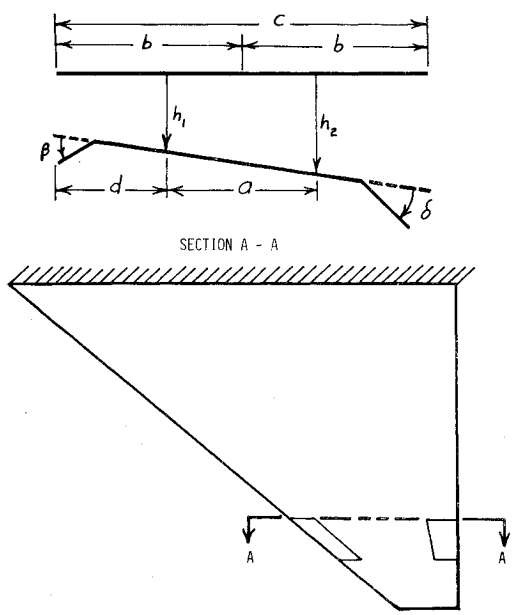

Fig. 1 Delta-wing model.

Received Nov. 3, 1976; revision received March 9, 1977.
Index category: Aeroelasticity.

*Professor, Department of Mechanical Engineering. Member AIAA.

of the motion of a lifting surface, b) leading and/or trailing-edge control surfaces, c) actuators for moving the control surfaces, and d) feedback control system components for processing the signals from the sensors.

The control surface deflection and velocity relationship between the control surface and the lifting surface motion is defined by a feedback control law. A mathematical programing method for finding an optimum control law which will suppress flutter and minimize the response of a lifting surface to a gust load will be presented here. The control law is assumed to have the form

$$\begin{Bmatrix} \beta \\ \delta \end{Bmatrix} = \begin{bmatrix} p_1 & p_3 \\ p_2 & p_4 \end{bmatrix} \begin{Bmatrix} h_1/b \\ \alpha \end{Bmatrix} + i \begin{bmatrix} p_5 & p_7 \\ p_6 & p_8 \end{bmatrix} \begin{Bmatrix} h_1/b \\ \alpha \end{Bmatrix}$$

$$= CL \begin{Bmatrix} h_1/b \\ \alpha \end{Bmatrix} \tag{1}$$

Where $i=\sqrt{-1}$. The P_i's are constant coefficients which must be determined in such a way that the system will have the desired flutter velocity, and the peak output power spectral density function of the angular response to a gust loading will be at a minimum for a specified freestream velocity. The deflections h_1 and α are assumed to be harmonic and are represented by the complex variables

$$\begin{Bmatrix} h_1/b \\ \alpha \end{Bmatrix} = \begin{Bmatrix} H_1 \\ H_2 \end{Bmatrix} e^{i\omega t}$$

where H_1 and H_2 are complex. The real part of h_1 and α represents the actual displacements. When these complex displacements are multiplied by i then the product is proportional to the derivatives of the displacements with respect to time; hence, the control law [Eq. (1)] specifies that the leading and trailing edge control surface displacements are linear functions of h, α, and their derivatives with respect to time.

It will be assumed that the wing motion at the h_1 and h_2 (see Fig. 1) locations are measured by linear accelerometers and the control law is mechanized as described in Ref. 7.

II. Flutter Analysis

The differential equations of motion of a three-dimensional lifting surface are obtained from Lagrange's equation of motion[7,9] by assuming that the unknown motion is described by a linear combination of the orthogonal modes (the undamped natural modes of the system) in the following manner:

$$h(x,y,t) = \sum_{i=1}^{n} q_i(t) Z_i(x,y) \tag{2}$$

If structural damping is neglected, then the equations of motion are

$$M_i \ddot{q}_i(t) + \omega_i^2 M_i q_i(t) = Q_i(t) \tag{3}$$

where

$$M_i = \int\int_s m(x,y) Z_i^2(x,y)\,dx\,dy \tag{4}$$

is the generalized mass, and

$$Q_i(t) = \int\int_s \Delta P(x,y,t) Z_i(x,y)\,dx\,dy \tag{5}$$

is the generalized aerodynamic force. The total pressure distribution $\Delta P(x,y,t)$ consists of contributions due to each flexible mode plus those due to the leading-edge and trailing-edge control surfaces. Hence,

$$\Delta P(x,y,t) = \sum_{j+1}^{n} \Delta P_j(x,y) q_j(t) + \Delta P_\delta \delta + \Delta P_\beta \beta \tag{6}$$

where ΔP_j is the pressure distribution due to each flexible mode, and ΔP_β and ΔP_δ are the pressure distributions due to leading and trailing edge controls, respectively. Substituting the expressions for M_i and Q_i into Eq. (3) and assuming that the system is undergoing harmonic oscillations, yields the following form of the equations of motion:

$$(-\omega^2 M_i + \omega_i^2 M_i) q_i(t) = \sum_{j=1}^{n} \left(q_j(t) \int\int_s \Delta P_j Z_i\,dx\,dy\right)$$

$$+\beta \int\int_s \Delta P_\beta Z_i\,dx\,dy + \delta \int\int_s \Delta P_\delta Z_i\,dx\,dy \tag{7}$$

where the inertia terms due to the control surface deflection are neglected.

In Ref. 7 it is shown that Eq. (7) may be expressed in the form

$$(-\omega^2 M_i + \omega_i{}^2 M_i) q_i(t) = \sum_{j=1}^{n} q_j \left(\int\int_s \Delta P_j Z_i\,dx\,dy \right.$$

$$\left. + (A_j + iB_j) \int\int_s \Delta P_\beta Z_i\,dx\,dy + (C_j + iD_j) \int\int_s \Delta P_\delta Z_i\,dx\,dy \right) \tag{8}$$

where the parameters A_i, B_i, C_i and D_i are given in Ref. (7) by the relations

$$A_i = Z_i(x_1,y_1)\left(\frac{P_1}{b} - \frac{P_3}{a}\right) + Z_1(x_2,y_2)\frac{P_3}{a} \tag{9a}$$

$$B_i = Z_i(x_1,y_1)\left(\frac{P_5}{b} - \frac{P_7}{a}\right) + Z_i(x_2,y_2)\frac{P_7}{a} \tag{9b}$$

$$C_i = Z_i(x_1,y_1)\left(\frac{P_2}{b} - \frac{P_4}{a}\right) + Z_i(x_2,y_2)\frac{P_4}{a} \tag{9c}$$

$$D_i = Z_i(x_1,y_1)\left(\frac{P_6}{b} - \frac{P_8}{a}\right) + Z_i(x_2,y_2)\frac{P_8}{a} \tag{9d}$$

where the nondimensional deflections of the wing at the sensors were given by relations:

$$\frac{h_1}{b} = \frac{1}{b}\sum_{i=1}^{n} q_i(t) Z_i(x_1,y_1),$$

$$\frac{h_2}{b} = \frac{1}{b}\sum_{i=1}^{n} q_i(t) Z_i(x_2,y_2) \tag{10}$$

and the angle of attack was approximated by the relation:

$$\alpha = (h_2/h_1)/a = \frac{1}{a}\sum_{i=1}^{n} [Z_i(x_2,y_2) - Z_1(x_1,y_1)] q_i(t) \tag{11}$$

Equation (8) may be written in the following matrix form

$$[C(M+A) - \lambda I]q = 0 \tag{12}$$

where

$$\lambda = 1/\omega^2 \tag{13}$$

$$C = \begin{bmatrix} 1/\omega_1^2 M_1 & & & \\ & 1/\omega_2^2 M_2 & & \\ & & \ddots & \\ & & & 1/\omega_n^2 M_n \end{bmatrix} \tag{14}$$

$$M = \begin{bmatrix} M_1 & & & \\ & M_2 & & \\ & & \ddots & \\ & & & M_n \end{bmatrix} \tag{15}$$

I is the identity matrix and A is a generalized aerodynamic force matrix whose components are:

$$A_{ij} = \frac{I}{\omega^2}\left(\int\int_s \Delta P_j Z_i \mathrm{d}x\,\mathrm{d}y + (A_j + iB_j)\int\int_s \Delta P_\beta Z_i \mathrm{d}x\,\mathrm{d}y + (C_j + iD_j)\int\int_s \Delta P_\delta Z_i \mathrm{d}x\,\mathrm{d}y\right) \tag{16}$$

When λ is pure real then the system is undergoing neutral steady-state oscillations. When λ is complex and the imaginary part is positive, then the system has negative damping and is unstable (flutter occurs), when the imaginary part of λ is negative the system has positive damping and the system is stable.

III. Gradient Search for the Flutter Velocity Constraint

A gradient search procedure may be used to find the control law parameters which provide for neutral steady-state oscillation of the wing-feedback-control-system at a specified freestream velocity. This freestream velocity will be called the flutter velocity constraint V_c. The control law coefficients which are determined in the gradient search will not necessarily be the optimum coefficients which minimize the response of the wing to a gust loading at a specified freestream velocity V_g which will be less than V_c.

The gradient search subroutine requires the derivatives of the flutter velocity with respect to the control coefficients. These derivatives are found by considering the equation:

$$V = b\omega/k \tag{17}$$

The partial derivative of V with respect to a coefficient P_j, may be found by differentiating Eq. (17), i.e.,

$$\frac{\partial V}{\partial P_j} = -\frac{b\omega^3}{2k}\frac{\partial \lambda}{\partial P_j} \qquad j = 1,2,\ldots,8 \tag{18}$$

where $\lambda = 1/\omega^2$. The reduced frequency k is assumed constant in Eq. (17); however, it will change slightly during the course of a gradient search.

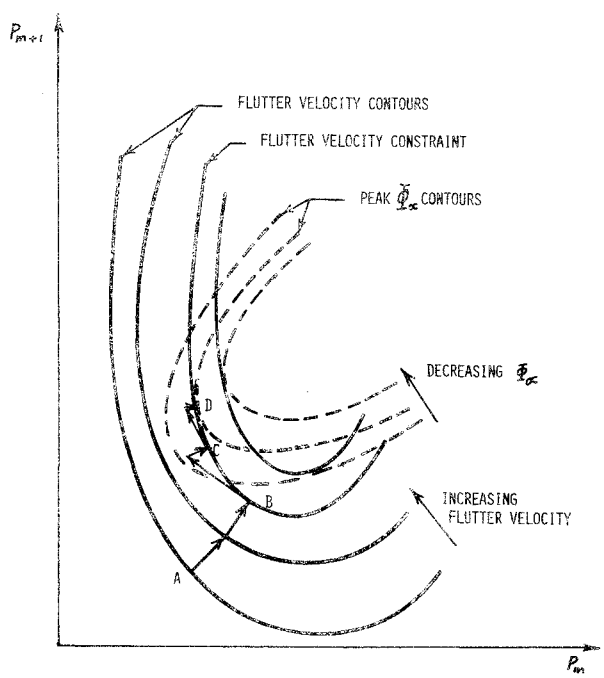

Fig. 2 Optimization path.

The derivatives $\partial V/\partial P_i$ $(i = 1,2,\ldots,8)$ are found by solving the following equations[10] for $\partial\lambda/\partial P_j$:

$$\left[\begin{array}{c|c} \bar{q}^T & 0 \\ \hline C(M+A) - \lambda I & -q \end{array}\right]\left\{\begin{array}{c} \partial q/\partial P_j \\ \hline \partial\lambda/\partial P_j \end{array}\right\} = \left[\begin{array}{c} 0 \\ \hline -C\partial A/\partial P_j \end{array}\right]\{q\} \tag{19}$$

Since $\partial q/\partial P_j$ and $\partial\lambda/\partial P_j$ are generally complex, let

$$\partial\lambda/\partial P_j = \partial\lambda_R/\partial P_j + i\partial\lambda_I/\partial P_j \tag{20}$$

where $\partial\lambda_R/\partial P_j$ and $\partial\lambda_I/\partial P_j$ are the real and imaginary derivatives respectively.

Since $\partial\lambda/\partial P_j$ will be complex then $\partial V/\partial P_j$ will be complex; hence, it is necessary to constrain the gradient search in such a way that the variation of the P_i's produce only a real variation of the flutter velocity.

Let

$$V = V_R + iV_I \tag{21}$$

be the complex flutter velocity. When the system is in a state of neutral stability, then $V_I = 0$. If the variations of P_i are such that the variations of P_i are such that the variations of V are pure real, then

$$\mathrm{d}V_I = \sum_{j=1}^{8}\frac{\partial V_I}{\partial P_j}\mathrm{d}P_j = 0 \tag{22}$$

The rate of change of V_R is

$$\frac{\mathrm{d}V_R}{\mathrm{d}s} = \sum_{j=1}^{8}\frac{\partial V_R}{\partial P_j}\frac{\mathrm{d}P_j}{\mathrm{d}s} \tag{23}$$

where s is a measure of distance along some line in the coordinate space formed by $P_1, P_2, \ldots, P_8$ and $\mathrm{d}P_i/\mathrm{d}s$ are the direction cosines which must obey the relationship

$$\sum_{j=1}^{8}\left(\frac{\mathrm{d}P_j}{\mathrm{d}s}\right)^2 = 1 \tag{24}$$

It is shown in Ref. 11, that the constrained variations of P_j are given by

$$P_j^{(n+1)} = P_j^{(n)} + \left(\frac{\partial V_R}{\partial P_j} + \phi\frac{\partial V_I}{\partial P_j}\right)s/\frac{\mathrm{d}V_R}{\mathrm{d}s} \tag{25}$$

where $P_j^{(n+1)}$ are the new coefficients and $P_j^{(n)}$ are the old coefficients,

$$\frac{\mathrm{d}V_R}{\mathrm{d}s} = \left[\sum_{i=1}^{8}\left(\frac{\partial V_R}{\partial P_i}\right)^2 + \frac{\partial V_R}{\partial P_i}\phi\frac{\partial V_I}{\partial P_i}\right]^{1/2} \tag{26}$$

and

$$\phi = -\sum_{j=1}^{8}\left(\frac{\partial V_I}{\partial P_j}\frac{\partial V_R}{\partial P_j}\right)/\sum_{j=1}^{8}\left(\frac{\partial V_I}{\partial P_j}\right)^2. \tag{27}$$

Let

$$\frac{\mathrm{d}V_R}{\mathrm{d}s} = \frac{V_c - V}{s} = \frac{\Delta V}{s} \tag{28}$$

where V is the flutter velocity corresponding to $P_i^{(n)}$. Then, upon substituting s from Eq. (28) into Eq. (25), it is seen that

$$P_j^{(n+1)} = P_j^{(n)} + \left(\frac{\partial V_R}{\partial P_j} + \phi\frac{\partial V_I}{\partial P_j}\right)\Delta V/\left(\frac{\mathrm{d}V_R}{\mathrm{d}s}\right)^2 \tag{29}$$

From Eqs. (18) and (20) it may be shown that

$$\frac{\partial V_R}{\partial P_j} = -(b\omega^2/2k)\frac{\partial \lambda_R}{\partial P_j} \tag{30}$$

and

$$\frac{\partial V_I}{\partial P_j} = -(b\omega^2/2k)\frac{\partial \lambda_I}{\partial P_j}\cdot \tag{31}$$

If Eqs. (30) and (31) are substituted into Eqs. (26) through Eq. (29) then:

$$P_j^{(n+1)} = P_j^{(n)} - (b\omega^2/2k)\left(\frac{\partial \lambda_R}{\partial P_j} + \phi\frac{\partial \lambda_I}{\partial P_j}\right)\Delta V/\left(\frac{dV_R}{ds}\right)^2 \tag{32}$$

where

$$\left(\frac{dV_R}{ds}\right)^2 = \left(\frac{b\omega^3}{2k}\right)^2 \sum_{i=1}^{8}\left[\left(\frac{\partial \lambda_R}{\partial P_i}\right)^2 + \frac{\partial \lambda_R}{\partial P_i}\phi\frac{\partial \lambda_I}{\partial P_i}\right] \tag{33}$$

and

$$\phi = -\sum_{j=1}^{8}\left(\frac{\partial \lambda_I}{\partial P_j}\frac{\partial \lambda_R}{\partial P_j}\right)/\sum_{j=1}^{8}\left(\frac{\partial \lambda_I}{\partial P_j}\right)^2 \tag{34}$$

Equation (32) may be used in an iterative manner to execute a gradient search (as from A to B of Fig. 2) such that the system will have a specified flutter velocity. The new coefficients $P_j^{(n+1)}$ will be pure real; however, the flutter velocity is a nonlinear function of the P_j's; hence, the velocity corresponding to the new coefficients may not be equal to V_c. If the gradient search is repeated, then the search will converge to V_c after several iterations provided ΔV is not excessively large. AΔV of five to ten percent of the initial flutter velocity is recommended. If larger increases in the flutter velocity are needed it may be achieved in several gradient searches of five to ten percent increments of the initial flutter velocity.

IV. Gust Response

The equation of motion for a lifting surface which is subjected to a gust loading may be written in the form of Eq. (3) where $Q_i(t)$ includes the integral of the gust pressure integrated over the surface. If the gust pressure is assumed to be a simple harmonic, then

$$\Delta P_g = \Delta p_g e^{i\omega_g t} \tag{35}$$

The response of the system will be simple harmonic; thus,

$$q_i(t) = U_i e^{i\omega_g t} \tag{36}$$

Equation (3) may be expressed in the matrix form

$$[-\omega_g^2(M+A)+K]\{U\} = \{G\} \tag{37}$$

where K is the inverse of C, the square matrices C, M, and A are given by Eqs. (14-16), respectively, $\{G\}$ is the gust load vector whose components are given by the relation

$$G_i = \int\int_s \Delta p_g(x,y,t)Z_i(x,y)\,dx\,dy \tag{38}$$

The components U_i of the vector $\{G\}$ may be found by solving Eq. (37). The response of the lifting surface at any point may then be found by substituting U_i from Eq. (37) into Eqs. (36) and then substituting the results into Eq. (2), and the angle of attack may be computed from Eqs. (11).

It has been shown[12] that the input-output relation of the power spectral density functions for the response of airplanes to atmospheric turbulence may be written in the form

$$\Phi_\alpha(\omega_g) = |\bar{\alpha}|^2\Phi_{w_g}(\omega_g) \tag{39}$$

The response α is computed for a unit input disturbance over a range of frequencies from zero to large values for which there is an appreciable response.

The von Karman generalized power spectrum for transverse components of turbulence was assumed, it may be expressed as

$$\frac{\Phi_{w_g}(\omega_g)}{\sigma_{w_g}^2} = \frac{[1+8/3(1.339k)^2]/\pi}{[1+(1.339k)^2]^{11/6}} \tag{40}$$

where $k = \omega L/V_g$. And

$$\sigma_{w_g}^2 = \int_0^\infty \Phi_{w_g}(\omega_g)\,d\omega_g \tag{41}$$

Typical curves for the power spectral density functions and the frequency response squared are shown in Fig. 3. From these curves it is seen that the peak of the output power spectral density function may occur at a different f than the f of the peak value of the frequency response.

V. Gust Response Minimization

A method for minimizing the peak of the output power spectral density function Φ_α will be presented next. Φ_α may be minimized in a gradient search along a constant flutter velocity hypersurface as shown from B to D in Fig. 2. If the search deviates excessively from the desired flutter velocity then a gradient search for the desired flutter velocity is executed as at point C. An alternate search scheme was tried which used the inequality constraint $V_R \geq V_c$ and a gradient search to minimize Φ_α; however, this scheme produced values of Φ_α which were consistently greater than the values given by the method described above. This may indicate that the flutter velocity contours and the Φ_α contours are more complex than envisioned in Fig. 2.

Since the search for a minimum peak Φ_α will be along a tangent to a constant velocity hypersurface when the equality constraint $V_R = V_c$ is imposed, a gradient projection search may be used. The optimization problem is then:

$$\text{Minimize: } \Phi_\alpha = \Phi_\alpha(P_1, P_2, \ldots P_8)$$

$$\text{Subject to: } V_R = V_c, V_I = 0 \tag{42}$$

It is shown in Ref. 11 that for a search of this type new values of P_j may be computed from the relation:

$$P_j^{(n+1)} = P_j^{(n)} + \left(\frac{\partial \Phi_\alpha}{\partial P_j} + \psi_R\frac{\partial V_R}{\partial P_j}\cdot\psi_I\frac{\partial V_I}{\partial P_j}\right)S/2\psi_0 \tag{43}$$

where ψ_R and ψ_I are found by solving the following linear equations

$$\psi_R\sum_{i=1}^{8}\left(\frac{\partial V_R}{\partial P_i}\right)^2 + \psi_I\sum_{i=1}^{8}\frac{\partial V_R}{\partial P_i}\frac{\partial V_I}{\partial P_i} = -\sum_{i=1}^{8}\frac{\partial V_R}{\partial P_i}\frac{\partial \Phi_\alpha}{\partial P_i} \tag{44}$$

$$\psi_R\sum_{i=1}^{8}\frac{\partial V_R}{\partial P_i}\frac{\partial V_R}{\partial P_i} + \psi_I\sum_{i=1}^{8}\left(\frac{\partial V_I}{\partial P_i}\right)^2 = -\sum_{i=1}^{8}\frac{\partial V_I}{\partial P_i}\frac{\partial \Phi_\alpha}{\partial P_i}$$

and S is an arbitrary step size which must be found by trial.

Values in Eqs. (43) and (44) are computed at a gust frequency f corresponding to the peak Φ_α.

The derivatives $\partial\phi_\alpha/\partial P_i$ may be found by differentiating Eqs. (39), i.e.

$$\frac{\partial \phi_\alpha}{\partial P_i} = 2\left(\alpha_R\frac{\partial \alpha_R}{\partial P_i} + \alpha_I\frac{\partial \alpha_I}{\partial P_i}\right)\phi_{w_g} \tag{45}$$

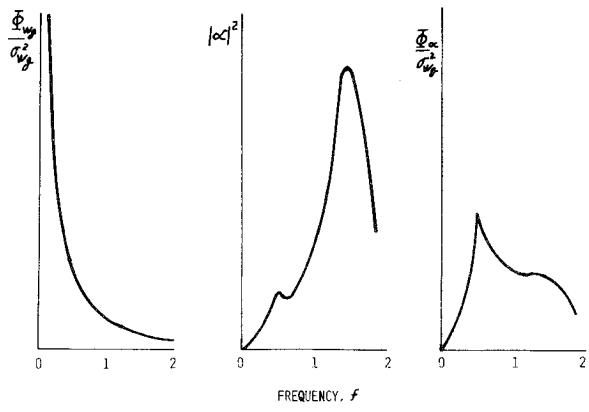

Fig. 3 Input and output power spectral density functions.

where α_R and α_I are the real and imaginary parts of α respectively. The derivatives of α_R and α_I may be found by differentiating Eqs. (11):

$$\frac{\partial(\alpha_R + i\alpha_I)}{\partial P_f} = \frac{1}{a}\sum_{i=1}^{n}(Z_i(X_2 Y_2) - Z_i(X_1 Y_1))\frac{\partial q_i}{\partial P_i} \tag{46}$$

where $\partial q_i/\partial P_i$ are in turn found by differentiating Eqs. (36) and (37) to find

$$\frac{\partial q_i}{\partial P_i} = \frac{\partial U_i}{\partial P_i} e^{i w_g t} \tag{47}$$

and

$$[-\omega_g^2(M+A)+K]\{\frac{\partial U}{\partial P_i}\} - \omega_g^2 \frac{\partial A}{\partial P_i}\{U\} = 0 \tag{48}$$

where Eqs. (48) must be solved for $\partial U/\partial P_i$. The derivatives $\partial V_R/\partial P_i$ and $\partial V_I/\partial P_j$ may be found from Eqs. (46, 30, and 31).

The peak value of ϕ_α may be found by first finding the maximum value of ϕ_α and its corresponding gust frequency f^* by computing ϕ_α for gust frequencies $F=\Delta f,\ 2\Delta f,\ \ldots, n\Delta f$, where $n\Delta f$ is some arbitrary large value of f where ϕ_α is small. Next, a Golden Section search may be used to find a more accurate maximum value of ϕ_α in the interval $f^* - \Delta f < f < f^* + \Delta f$. $P^{(n+1)}$ must be evaluated for a frequency f which corresponds to the peak value of ϕ_α.

Peak output responses for β, δ or $h(x,y)$ may be minimized by replacing α with either β, δ or h in Eqs. (39, 42-44).

For a Gaussian process the average frequency of exceeding a response peak of level z is [12]

$$N(z) = N_{o,z} e^{-z/(2\sigma_z^2)} \tag{49}$$

where

$$N_{o,z} = \frac{1}{2\pi}\left[\frac{\int_0^\infty \omega_g^2 \Phi_z(\omega_g)\,d\omega_g}{\sigma_z^2}\right]^{1/2} \tag{50}$$

The mean-square value of the response z is

$$\sigma_z^2 = \int_0^\infty \Phi_z(\omega_g)\,d\omega_g \tag{51}$$

The response z may be any of the responses α, β, δ, or h.

$N(z)$ or σ_z^2 may be minimized by substituting $N(\kappa)$ or σ_z^2 for Φ_α in Eqs. (42) through (44). The functions $N_{o,z}$, σ_z^2 and their derivatives with respect to P_i may be evaluated by numerical quadrature for a range of ω_g from zero to large values for which there is an appreciable response.

It should be noted that minimizing the peak output response does not necessarily mean that the response will be minimized over the entire frequency range or that σ_z^2 or $N(z)$ will be minimized. Conversely, the minimization of σ_z^2 or $N(z)$ does not mean that the response will be minimized at every frequency over the range, or that the peak output response will be minimized. However, it may be possible to minimize $N(z)$ with Φ_z constrained to be less than or equal to some maximum value, or to minimize the peak value of ϕ_z with $N(z)$ constrained.

VI. Numerical Results

The optimization procedures which were described in the previous section were used to optimize the active control system for the simplified delta wing which was described in Ref. 7. Values of the generalized forces were supplied by I. Abel of the NASA Langley Research Center for a range of reduced frequencies and Mach numbers. A cubic spline was used to interpolate the data for arbitrary reduced frequencies between 0.2 and 1.2 with the Mach number equal to 0.9. The atmospheric density was assumed to be 6.51×10^{-8} lb-sec^2/in.^{4} (6.96×10^{-4} gm/cm^3) and a scale of turbulence L was assumed to be 2500 ft (762 m).

A. Open-Circuit Response

When all of components of the control law are zero then the deflections of the leading-edge (LE) and trailing-edge (TE) control surfaces will be zero for any response of the lifting surface. This corresponds to an open circuit or open-loop feedback control system in which the control surfaces are constrained to zero deflections.

The open circuit flutter velocity was computed to be 139.4 m/sec (5490 in./sec). The peak value of the output response ϕ_α to a harmonic gust input and the corresponding gust frequencies are given in Table 1 for two different freestream velocities.

B. Response Suppression

The output response ϕ_α of the lifting surface to a sinusoidal gust input may be suppressed by minimizing ϕ_α while the flutter velocity is held constant. With the flutter velocity constraint set equal to the open-circuit flutter velocity, ϕ_α was minimized first with only the trailing-edge control surface active and then with the leading-and trailing-edge surfaces active.

The optimum control law found with only the trailing-edge control surface (TE) active was:

$$CL = \begin{bmatrix} 0 & 0 \\ -0.6086 & 1.930 \end{bmatrix} + i\begin{bmatrix} 0 & 0 \\ 3.079 & -4.817 \end{bmatrix}$$

The optimum control law found with both the leading-edge and the trailing-edge control surfaces (L&TE) active was:

$$CL = \begin{bmatrix} 0.5682 & -2.925 \\ -1.740 & 4.298 \end{bmatrix} + i\begin{bmatrix} 4.996 & 1.726 \\ 4.506 & -0.5937 \end{bmatrix}$$

The peak output responses ϕ_α, and the corresponding frequencies and control surface deflections are given in Table 2.

It is seen from Tables 1 and 2 that a 50.7% reduction of ϕ_α has been achieved with only the trailing-edge control active and a 64.9% reduction was achieved with both the leading- and trailing-edge controls active.

Table 1 Open-circuit responses and frequencies

Flutter velocity (m/sec)	Freestream velocity (m/sec)	ϕ_α, [(deg/{m/sec})^2/rad/sec]	f (Hz)
139.4	111.6	1.270×10^{-4}	9.943
139.4	117.1	1.866×10^{-4}	10.19

Table 2 Optimum gust response with the freestream velocity equal to 111.6 m/sec

Active controls	Flutter velocity[a] (m/sec)	ϕ_α [(deg/{m/sec})^2/rad/sec]	f (Hz)	β deg/m/sec	δ deg/m/sec
TE	139.4	0.6260×10^{-4}	9.977	0	5.157
L&TE	138.4	0.4452×10^{-4}	10.12	20.54	9.366

[a] A one percent deviation from the flutter velocity constraint was allowed during gust response minimization procedure.

Table 3 Unoptimized gust response after gradient search

Active	Flutter velocity (m/sec)	Freestream velocity (m/sec)	ϕ_α [(deg/{m/sec})^2/rad/sec)]	f (Hz)	β deg/m/sec	δ deg/m/sec
TE	146.4	111.6	0.3333×10^{-4}	10.39	0	8.724
TE	146.4	117.1	0.4669×10^{-4}	10.64	0	9.527
L&TE	146.5	111.6	0.3193×10^{-4}	10.40	2.796	8.547
L&TE	146.5	117.1	0.4438×10^{-4}	10.65	3.035	9.279

C. Gradient Velocity Search

The gradient velocity search was used to increase the flutter velocity constraint by 5% from 139.4 m/sec to 146.4 m/sec. The control laws at the end of the gradient search were:

$$CL=\begin{bmatrix}0 & 0\\ 1.154 & -0.1231\end{bmatrix}+i\begin{bmatrix}0 & 0\\ 1.763 & 1.136\end{bmatrix}$$

for the trailing edge active and

$$CL=\begin{bmatrix}-0.4675 & -0.01551\\ 1.167 & -0.1254\end{bmatrix}+i\begin{bmatrix}-0.5153 & -0.3796\\ 1.777 & 1.157\end{bmatrix}$$

for the leading and trailing edge active.

The peak output responses of ϕ_α, and the corresponding frequencies and control surface deflections at the end of the gradient search are given in Table 3.

It should be observed from Tables 1 and 3 that when the flutter velocity was increased by means of the gradient velocity search the output response ϕ_α was reduced by 73% or more in each case.

D. Optimized Gust Response at End of Gradient Velocity Search

After the desired flutter velocity of 146.4 m/sec was achieved in Sec. C, the output response ϕ_α was minimized with the flutter velocity constraint held equal to 146.4 m/sec.

The optimum control laws found were as follows:

$$CL=\begin{bmatrix}0 & 0\\ 0.7129 & -0.2848\end{bmatrix}+i\begin{bmatrix}0 & 0\\ 2.294 & 1.241\end{bmatrix}$$

for a freestream velocity of 111.6 m/sec, with only the trailing edge control surface active,

$$CL=\begin{bmatrix}0 & 0\\ 0.6336 & -0.3421\end{bmatrix}+i\begin{bmatrix}0 & 0\\ 2.258 & 1.182\end{bmatrix}$$

for a freestream velocity of 117.1 m/sec with only the trailing edge control surface active,

$$CL=\begin{bmatrix}-0.8929 & -1.783\\ -1.353 & 1.104\end{bmatrix}+i\begin{bmatrix}0.5476 & -0.9379\\ 3.496 & 2.737\end{bmatrix}$$

for a freestream velocity of 111.6 m/sec with both the leading and trailing edge control surfaces active, and

$$CL=\begin{bmatrix}-0.9710 & -1.994\\ -1.786 & 1.113\end{bmatrix}+i\begin{bmatrix}0.4600 & -1.179\\ 3.393 & 2.952\end{bmatrix}$$

for a freestream velocity of 117.1 m/sec with both the leading and trailing edge control surfaces active. The peak values of ϕ_α are shown in Table 4.

A comparison of Tables 3 and 4 will reveal that with the trailing edge active the optimum values of the peak ϕ_α are at least 15% less than the unoptimized values and the amplitude of the trailing edge control surface decreased slightly. With both the leading and trailing edge control surfaces active the peak value of ϕ_α decreased by at least 23%, but the amplitude of the leading edge control surface almost doubled as a result of the optimization procedure.

E. Gradient Velocity Search to 169.9 m/sec

The gradient search procedure was used to find the control law which would give a flutter velocity of 169.9 m/sec. No attempt was made to minimize the peak response since it occured at a reduced frequency less than 0.2, and generalized forces for reduced frequencies below 0.2 were not available. Extrapolated values of the generalized forces gave questionable values of ϕ_α. The values of the control law parameters at the end of the search were:

$$CL=\begin{bmatrix}0 & 0\\ 9.069 & -5.624\end{bmatrix}+i\begin{bmatrix}0 & 0\\ 8.915 & 1.054\end{bmatrix}$$

with the trailing edge control surface active, and

$$CL=\begin{bmatrix}-3.338 & 1.474\\ 8.900 & -5.217\end{bmatrix}+i\begin{bmatrix}-1.003 & -2.283\\ 6.841 & 3.309\end{bmatrix}$$

with both leading and trailing edge control surfaces active.

VII. Discussion

The numerical examples demonstrate that the gradient velocity search procedure is an effective method for finding a control law which will increase the flutter velocity. The gust

Table 4 Optimum gust response for a flutter velocity constraint of 146.4 m/sec

Active	Flutter velocity (m/sec)	Freestream velocity (m/sec)	ϕ_α [(deg/{m/sec})^2/rad/sec]	f (Hz)	β deg/m/sec	δ deg/m/sec
TE	147.9	111.6	0.2785×10^{-4}	10.35	0	8.480
TE	147.9	117.1	0.3946×10^{-4}	10.58	0	8.996
L&TE	147.9	111.6	0.2370×10^{-4}	10.24	4.465	8.980
L&TE	147.9	117.1	0.3398×10^{-4}	10.47	5.429	9.484

response minimization procedure appears to be very effective in minimizing the peak value of ϕ_α along a constant flutter velocity hypersurface, in each case the procedure reduced the peak ϕ_α by a significant amount. It is possible that the optimum control laws found were local optima rather than global optima.

The numerical results show that the optimum control law changes with the freestream velocity. It is reasonable to assume that the control law will be different for each flight configuration, this suggests the need of an active control system which could adjust the control law with changing flight conditions.

The numerical results show that the leading and trailing edge active control system is more effective in reducing the peak ϕ_α than the trailing edge only system.

Acknowledgment

This research was supported by NASA Research Grant NSG 1125. The author wishes to thank I. Abel of the NASA Langley Research Center for his assistance and valuable suggestions during the course of this work.

References

[1]Thompson, G. O. and Kass, G. J., "Active Flutter Suppression—An Emerging Technology," *Journal of Aircraft*, Vol. 9, March 1972, pp. 230-235.

[2]Hodges, G. E., "Active Flutter Suppression—B52 Controls Configured Vehicle," AIAA Paper 73-322, Williamsburg, Va., 1973.

[3]Arnold, J. I. and Thompson, G. O., "B-52 Controls Configured Vehicle System Design," AIAA Paper 72-869, Stanford, Calif., 1972.

[4]Nissim, E., "Flutter Suppression Using Active Controls Based on the Concept of Aerodynamic Energy," NASA TN D-6199.

[5]Cwach, E. and Stearman, R. O., "Suppression of Flutter of Interfering Lifting Surfaces by the Use of Active Controls," AIAA Paper 74-404, Las Vegas, Nev., 1974.

[6]Nissim, E., "Active Flutter Suppression Using Trailing-Edge and Tab Control Surfaces," *AIAA Journal*, Vol. 14, June 1976, pp. 759-762.

[7]Sanford, M. C., Abel, I., and Gray, D. L., "A Transonic Study of Active Flutter Suppression Based on an Aerodynamic Energy Concept," *Journal of Aircraft*, Vol. 12, Feb. 1975, pp. 72-77.

[8]Griffin, K. E., "Flutter Characteristics and Feedback Suppression Results for Two Modes on Interference Lifting Surface Flutter," Master's Thesis, University of Texas at Austin, May 1972.

[9]Bisplinghoff, R., Ashley, H., and Halfman, R., *Aeroelasticity*, Addison-Wesley, Reading, Mass., 1955, pp. 122-124.

[10]Rudisill, C. S. and Chu, Y., "Numerical Methods for Evaluating the Derivatives of Eigenvalues and Eigenvectors," *AIAA Journal*, Vol. 13, June 1975, pp. 834-837.

[11]Beveridge, G. D. G. and Schecter, R. S., *Optimization Theory and Practice*, 1st ed., McGraw-Hill, New York, 1970, pp. 421-438.

[12]Pratt, K. G., "Response of Flexible Airplanes to Atmospheric Turbulence," *Performance and Dynamics of Aerospace Vehicles*, NASA SP-258; L-6892, 1971, pp. 439-503.